

## Behaviour of Radio-Thermoluminescence (X-Ray Irradiated), Thermal and Structural Characterization of Limestone

Mehmet İsmail Kati <sup>1\*</sup> 

<sup>1</sup> Experimental Science Applications and Research Center, Manisa Celal Bayar University, Manisa, Türkiye

\* [mehmetismailkati@gmail.com](mailto:mehmetismailkati@gmail.com)

\* Orcid: 0000-0002-9225-730X

Received: 21 April 2022

Accepted: 1 December 2022

DOI: 10.18466/cbayarfbe.1106810

### Abstract

This study reported radioluminescence properties of limestone from Kütahya, Türkiye, for the first time, which has been the subject of many studies in both mineralogical and gemological fields. Limestone is the general name of carbonate rocks, which is the mineral with typical colors according to the impurity elements in rock and exhibited luminescence properties under x-ray irradiation. The radio&thermoluminescence data were analyzed for limestone. Besides, x-ray diffraction pattern was created for structural characterization, scanning electron microscope images and energy dispersive x-ray spectroscopy maps were taken to determine morphological features. When the radioluminescence spectrum of the limestone was detailed, a broad emission consisting of several peaks was observed in the visible region. In the thermoluminescence spectrum taken after the x-ray excitation of the limestone, three thermoluminescence peaks were observed at 97 °C, 170 °C and 320 °C. Also; TL kinetic parameters are reported; The activation energy (E) and frequency factor (s) of the first peak were determined in detail using the methods of peak shape and varying heating rates.

**Keywords:** Limestone, radioluminescence (RL), thermoluminescence (TL), CaCO<sub>3</sub>.

### 1. Introduction

Limestone is one of the abundant minerals in nature. Generally, limestones consist of shells and animal skeletons found in shallow and warm seawater. Limestone formed in this way is a biological sediment. It can also be formed by direct evaporation or precipitation of calcium carbonate. Limestone, which is formed as a result of evaporation and precipitation, is a chemical sedimentary rock and is less common in nature than biological sedimentary rock[1]. Limestone can be found in various forms such as calcite, vaterite and aragonite under the main chemical formula CaCO<sub>3</sub>.

Calcite is a carbonate mineral and is the most structurally stable polymorph of calcium carbonate (CaCO<sub>3</sub>). Calcite, whose crystal system is generally hexagonal, can be seen in different crystal forms. More than 800 crystal forms are described in the literature[2]. Although it shows widespread twinning, it is twinning according to two different laws. In the first, the twin plane is the basal pinacoid, and in the second, the rhombohedral surface. Colorless or white when pure; It can also be observed in gray, yellow, brown, red, green,

blue and black colors depending on the impurity elements it contains. The most obvious distinguishing feature is that it can be dissolved by foaming very quickly with HCl [3]. Calcite, which is one of the most abundant minerals in nature, is the main component of carbonate sedimentary rocks (limestones), metamorphic rocks (marbles) and stalactites & stalagmites in travertines[4,5].

Aragonite is a carbonate mineral, one of the three most common crystal forms of calcium carbonate. It is widely known that they complete their physical formation with precipitation, regardless of fresh or saltwater environment[6]. The non-twinning types of aragonite, which has an orthorhombic crystal system, are rarely acicular and sometimes plate-shaped. It differs from calcite by its crystalline form and high specific gravity. Aragonite, which has a vitreous and resinous luster, is not as common as calcite. It is formed together with gypsum bands formed near the surface. Along with secondary minerals such as malachite and smithsonite in the oxidation zones of the mine deposits; It can occur in different metamorphic and sedimentary rocks [7].

Although nature is often found, there are only a few studies in the literature regarding the luminescence of limestone and its potential applications [8,9]. On the other hand, studies (dating, dose response, etc.) for calcite, which is a type of calcium carbonate, are much more due to its good luminescence response [10–14]. There are few studies examining the RL of calcite in the literature [15–18]. This study reported radioluminescence properties of limestone from Kütahya, Türkiye for the first time.

In the study, the structure characterization and luminescence behavior of the limestone extracted from *Kütahya-Tavşanlı (Aslan Baba region- near Merkez Karaköy village)* were investigated. Aslan Baba territory; although it is known by the local people, it is name of region in the triangle of Ağaköy, Başköy and Merkez Karaköy villages in Tavşanlı.

## 2. Materials and Methods

The limestone sample was extracted from the stream bed, whose location is given in Figure 1(a), using a mining hammer. The sample was cleaned with ethyl alcohol and dried in the sun in order to remove the physical and natural impurities on it. For X-ray diffraction (XRD) and Fourier transform infrared (FT-IR) analysis, a part of the sample was crushed and ground in a ball mill for 2 hours and powdered. The limestone sample was cut in dimensions 3x3x3 mm to make it for RL and TL measurements. Before all luminescence measurements, the sample was annealed at 500 °C for 30 minutes in order to eliminate the excitations that occur on the sample due to natural radiation (daylight, physical effects, etc.).

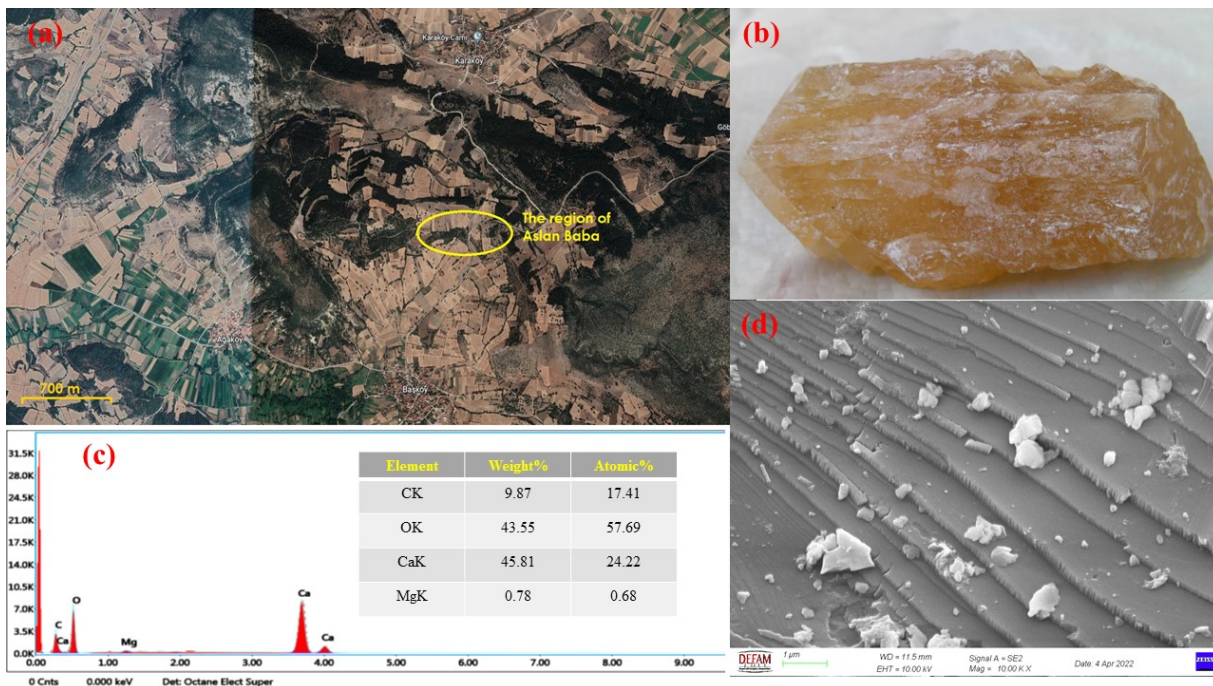


**Figure 1.** (a) The region of Aslan Baba in the map of Tavşanlı. (b) Untreated form of the limestone used in this study. (c) Energy dispersive X-ray spectroscopy (EDS) and (d) SEM image of limestone.

The description of sample X-ray diffraction pattern and phase analyses work performed was given in our previous work in detail[19]. For the RL measurements of the cast limestone sample, excitation was made with a Machlett OEG-50A X-ray tube operated at maximum 30 kV and 15 mA experimental conditions. Unlike Cathodoluminescence (CL), X-ray is used instead of electrons in RL, which is a very useful method for detecting defects in minerals[20]. Radioluminescence provides spectral data with curvature accuracy (repeatable data is obtained as data) by volumetric excitation of the sample from beginning to end, system

setup and data collection are relatively difficult. The radioluminescence emissions of the limestone were measured and recorded on a high-sensitivity wavelength multiplex CCD (Charge Coupled Device) detector capable of sensing between 275 and 995 nm. Before TL measurements, the sample was stimulated for various times with an x-ray source, which is a part of the RL, and TL spectra were taken with RA94 Reader/Analyzer TL equipment in the dark room. TL spectra of limestone were recorded under nitrogen atmosphere in the range of 50-400 °C at various heating rates.

Powdered limestone placed in potassium bromide was turned into pellets and the FT-IR spectrum was recorded for absorbance in the 580–2500  $\text{cm}^{-1}$  region using a Perkin Elmer Spectrum BX FT-IR Spectrometer at room temperature.

The thermal analysis (TG-DTA) of the sample was performed in the range of 25–1000  $^{\circ}\text{C}$ . The thermal analysis data obtained with the Hitachi SII Exstar 7300 device were recorded in the air atmosphere and with a heating rate of 10 $^{\circ}\text{Cmin}^{-1}$ . For the SEM photographs and EDS maps of the limestone, assistance was obtained from the Carl Zeiss Gemini 500 equipment and the edax unit in high vacuum. The samples were coated with Au/Pd alloy before being placed under vacuum.

### 3. Results and Discussion

#### 3.1. XRD Pattern of Limestone

In the analysis at room temperature, the XRD pattern and phase analysis results of the limestone compared with the ICSD 98-004-0107 standard pdf card are given in Figure 2 and Table 1.

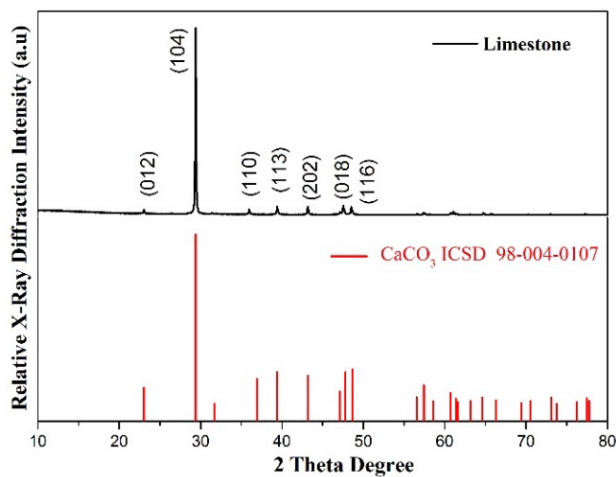


**Figure 2.** XRD pattern of limestone and standard pdf card.

Phase analysis results of the high score plus program on the XRD pattern of the limestone showed planes such as (104), (012), and (110) compatible with the *Calcium Carbonate* ( $\text{CaCO}_3$ ) phase. The crystallite size of the sample was calculated using the Scherrer formula ( $D=K\lambda/B\cos\theta$ ). Where K is space constant (0.94),  $\lambda$  is wavelength of the X-ray used (1.5405  $\text{\AA}$  Cu-K $\alpha$ ), B is the full width at half maxima (FWHM) of pattern and D is the crystallite size. The crystallite size 55.663 nm was found in the calculation made for the orientation (104), which is the most intense peak in the XRD pattern. In addition, the calculated average crystallite size is 37.122 nm.

**Table 1.** Peak ID report of Limestone

$2\theta$	Phase ID	Height (%)	$d(\text{\AA})$	hkl
23.060	$\text{CaCO}_3$	9.4	3.853	012
29.405	$\text{CaCO}_3$	100	3.035	104
35.981	$\text{CaCO}_3$	14.8	2.494	110
39.420	$\text{CaCO}_3$	18.8	2.284	113
43.172	$\text{CaCO}_3$	16.4	2.093	202
47.509	$\text{CaCO}_3$	19.3	1.912	018
48.514	$\text{CaCO}_3$	20.8	1.874	116

ICSD Card No: 98-004-0107

The crystal structure of the limestone was explained as the crystal system hexagonal, space group R-3c, space group number: 167 and lattice parameters of sample was calculated from XRD data. Lattice parameters calculated for limestone with hexagonal structure: (a 4.9880 $\text{\AA}$ ), (b 4.9880) and (c 17.0610). Besides, the unit cell volume and angles were found as 367.61 $\times 10^6\text{pm}^3$  and  $\alpha:90^{\circ}$ ,  $\beta:90^{\circ}$   $\gamma:120^{\circ}$ , respectively.

#### 3.2. FT-IR Spectrum of Limestone

The Fourier transform-IR survey was mainly conducted in the 580–200  $\text{cm}^{-1}$  range to collect qualitative information on the powdered limestone sample ( $\text{CaCO}_3$  for its chemical form) and possible unknown organic-inorganic components. Characteristic transmittance peaks of calcite and aragonite, which are  $\text{CaCO}_3$  group minerals, are observed in the FTIR spectrum of the limestone. This is an expected situation. Apart from these characteristic peaks in the spectrum, there are vibration peaks originating from atmospheric  $\text{CO}_2$  in the range of 2300–2400  $\text{cm}^{-1}$ .

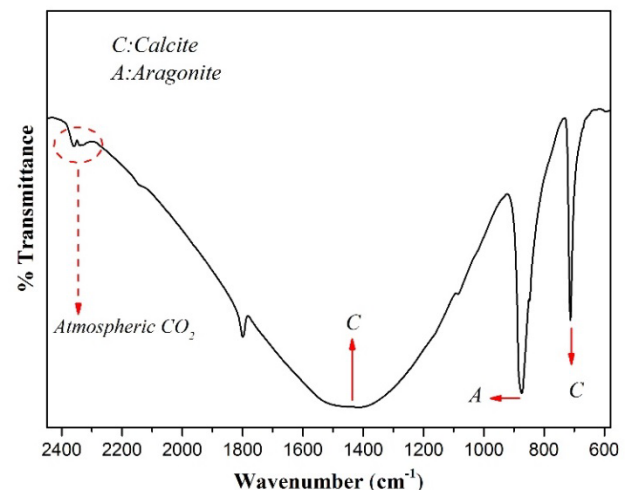


**Figure 3.** FT-IR spectrum of limestone.

In Figure 3, the characteristic peak positions of calcite are between 1370–1390, at 870 and 711  $\text{cm}^{-1}$ ; these bands are generally attributed to asymmetric stress modes and asymmetric and symmetric vibrations of the carbonate group, respectively. Characteristic vibration modes for aragonite are out-of-plane bending at 854  $\text{cm}^{-1}$  and asymmetric stress peaks at 1432  $\text{cm}^{-1}$  [19,21].

### 3.3. Thermal Analysis of Limestone

Thermal properties of powdered limestone were determined by using the Thermal Analysis-Thermal Gravimetry (DTA-TG) device. Figure 4. shows TG, DTA and DTG curves of powder limestone.

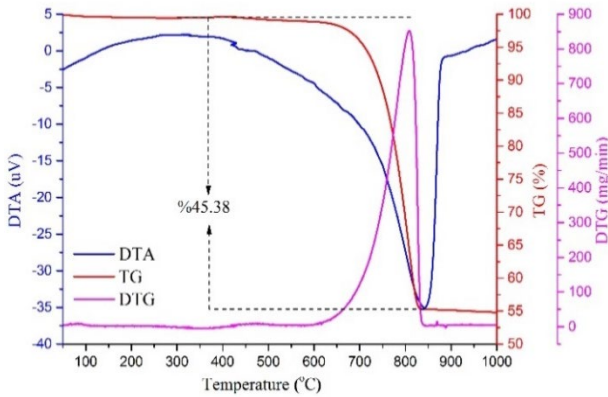


**Figure 4.** TG, DTA and DTG curves of the limestone.

15.2 milligrams of powdered sample was weighed and heated in a controlled nitrogen atmosphere from room temperature to 1000°C at a heating rate of 10°C/min. While there was no mass loss up to 400 °C, as it can be

clearly seen from the TG curve, when the temperature reached 900 °C, 45.38% of the sample mass was lost due to CaCO<sub>3</sub> decomposition[22]. This decomposition reaction started at approximately 485 °C, reached its peak at 807 °C and ended at 848 °C. No change was observed in the TG and DTG signals for the sample at temperatures above 900 °C.

### 3.4. SEM-EDS Images and Mapping of Limestone

SEM images were taken and energy dispersive x-ray spectroscopy analysis was performed to determine the morphology and composition of the limestone. SEM images allowed the morphological structure of the limestone to be observed, while at the same time allowing the composition of the image to be reached. In the images taken from different parts of the sample, it is seen that the calcium carbonate phase has a layered structure (Fig. 1d). In addition, a small amount of Mg impurities were found in the EDS analysis (Fig. 1c and Fig 5). Figure 5 shows a SEM image of the limestone, the EDS spectrum and the map of the composition in this region. While creating the maps of the elements, an ROI (Region of Interest) is determined for the characteristic X-ray energy of each element, and the signals at the border of this ROI are considered as verified data.

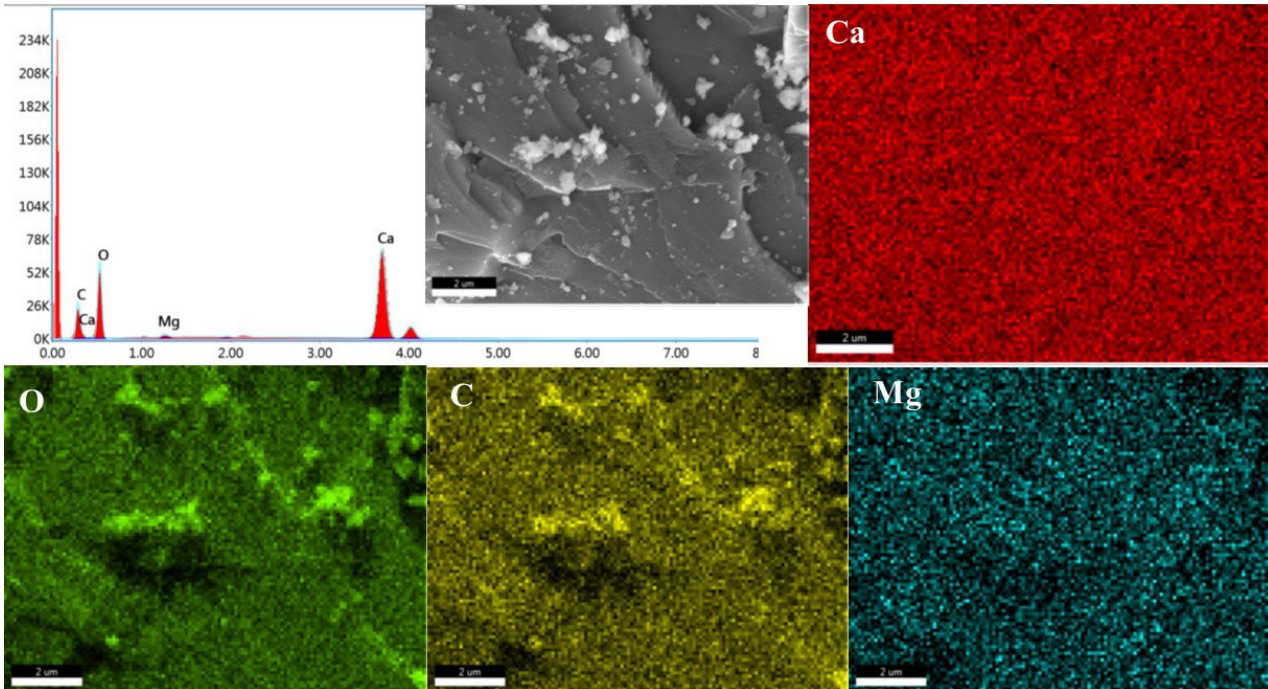


**Figure 5.** EDS mapping for SEM image of limestone.

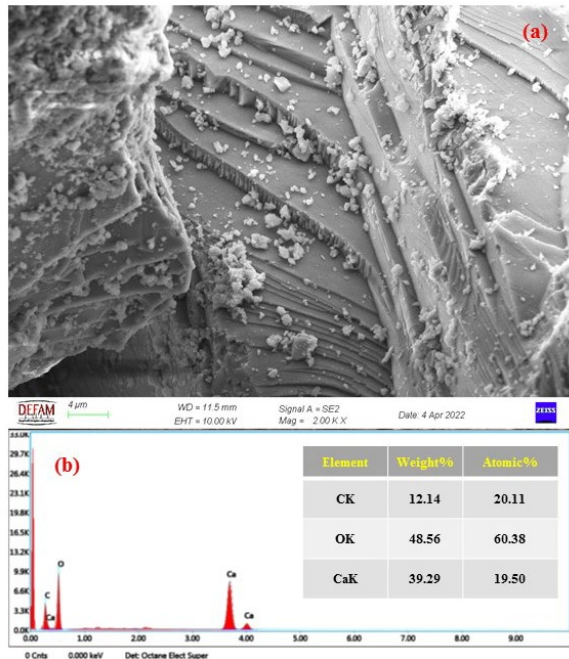


Figure 6. SEM image and EDS spectrum of limestone.

### 3.4. Radioluminescence Results of Limestone

The RL spectrum of the limestone taken in the range of 275-950 nm is shown in Figure 7. The general principle of the RL system is that it detects the emissions generated in the sample irradiated by X-ray excitation volumetrically. The RL spectrum of the sample consists of major peaks of 522 and 340 nm, the most intense at 627 nm, and minor peaks below these peaks.

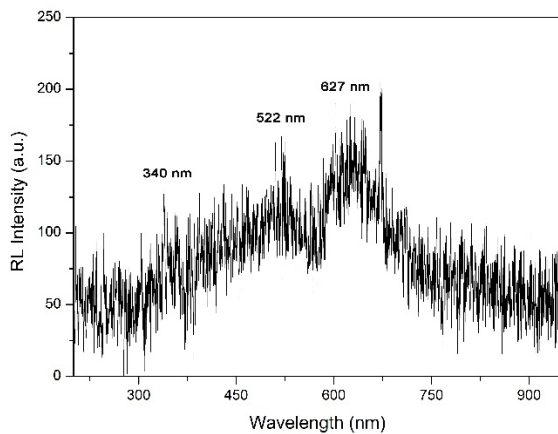


Figure 7. RL spectrum of limestone.

The dominant peak in this spectrum, 627 nm, is attributed to the  $4f^2 \rightarrow 6g^2G$  transitions of  $C^{1+}$ . The peak at 340nm corresponding to the transition of  $4s[1^{1/2}]^0 \rightarrow 4p[1/2]$  for  $Ca^{3+}$  ion. In addition, the  $3p^3P^0 \rightarrow 4s^3S$  transition at 522 nm for  $Mg^{1+}$ , which is the trace element in the sample, is seen in the RL spectrum[23].

### 3.5. Thermoluminescence Results of Limestone

In the thermoluminescence technique, unlike the radioluminescence, the sample is excited with the help of an excitation source (alpha, beta, x-ray, gamma-ray, daylight, etc.) before the analysis. Thus, electrons in the valence band move to the conduction band, the sample loses its stable structure and tends to return to its initial state. In the next stages, the electron leaving the conduction band sets out to return to the valence band and merge with the gap it created before. In this journey, the electron is trapped in the forbidden energy region between the valence band and the conduction band. The reason for the trap is the impurities and structure disorders in the sample. The glow that occurs as a result of the electrons getting rid of these traps and combining with the holes ( this region is called the recombination center) by means of temperature is called thermoluminescence[24].

TL technique is mostly used for reading personal dosimeters and dating historical objects (a wide range of cave stalactites and stalagmites, dinosaurs, mammoths, seashells).

For TL measurements, limestone was specially cut, exposed by X-ray at different times, and glow curves were created at varying heating rates. Figure 8 shows the TL glow curve obtained with the heating rate  $7^\circ C/s$  of the limestone exposed to x-rays for 10 minutes. There are three TL peaks in total around 170 and  $320^\circ C$ , with the highest peak at  $97^\circ C$ .

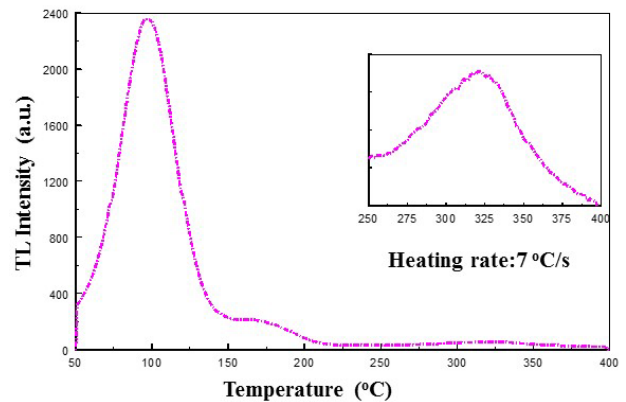
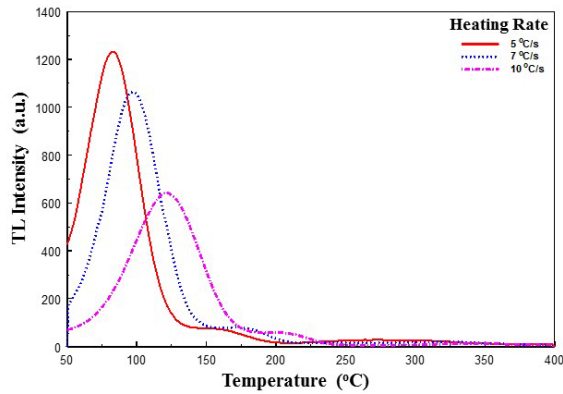


Figure 8. TL glow curve of limestone.

The sample was exposed to constant x-ray for 10 minutes and TL glow curves were obtained at varying heating rates. The glow curves obtained at different heating rates ( $5^\circ C/s$ ,  $7^\circ C/s$  and  $10^\circ C/s$ ) are shown in Figure 9.



**Figure 9.** The glow curves of the sample for varying heating rates.

It can be clearly seen from the figure that as the heating rate increased, the peak of the glow curve shifted towards higher temperatures. TL kinetic parameters were calculated by the peak shape method and the variable heating rate method developed based on this expected situation. The steps of calculating kinetic parameters using these two methods were explained in detail in our previous study[25–29]. The obtained activation energy frequency factor values are  $0.594 \pm 0.026$  eV and  $0.473 \pm 0.032$  eV,  $4.88 \times 10^6$  s<sup>-1</sup> and  $3.96 \times 10^6$  s<sup>-1</sup> for the peak shape and varying heating rates method, respectively.

#### 4. Conclusion

In the X-ray diffraction pattern and phase analysis of the limestone, no phase other than the hexagonal calcium carbonate phase was found. The trace element Mg was found and mapped in the EDS spectrum in some parts of the sample. Detailed information about the layered shell structure of the limestone was obtained with SEM images. It consists of many Gaussian peaks caused by impurity atoms that consist the main RL emission spectrum. Each of the components are emissions from the transition between levels and these emissions are explained. Activation energy values were calculated from the TL glow curves obtained. In further studies; It is planned to examine the dosimetric properties (dose response and fading, etc.) of limestone.

#### Author's Contributions

**Mehmet İsmail Katı:** Performed the experiment, result analysis and manuscript preparation.

#### Ethics

There are no ethical issues after the publication of this manuscript.

#### Acknowledgement

The experiments in this paper were partially performed at Manisa Celal Bayar University (Türkiye) - Experimental Science Applications and Research Center (DEFAM). I dedicate this article to my late grandfather Süleyman YAŞLI, whom I will always remember with gratitude.

#### References

- [1] J.M. Kalita, M.L. Chithambo, Thermoluminescence and infrared light stimulated luminescence of limestone (CaCO<sub>3</sub>) and its dosimetric features, *Applied Radiation and Isotopes*.154(2019)108888. doi:10.1016/j.aprad.20.108888.
- [2] P.D. Townsend, B.J. Luff, R.A. Wood, Mn<sup>2+</sup> transitions in the TL emission spectra of calcite, *Radiation Measurements* 23 (1994) 433–440. doi:10.1016/1350-4487(94)90076-0.
- [3] B. Şahin, H. Ağrılı, E. Koşun, H. Mengi, Mineraller, *MTA*, Ankara, 2008.
- [4] B. Yalçınalp, H. Ersoy, A. Firat Ersoy, C. Keke Öz, A. Kelimeler, Bahçecik (Gümüşhane) Travertenlerinin Jeolojik Ve Jeoteknik Özellikleri, *Jeoloji Mühendisliği Dergisi* 32(1) 2008.
- [5] İ. Çobanoğlu, B. Çelik, Evaluation of the use of an alternative mixture for pore filling material on travertine slabs, Special Issue of National Symposium on Engineering Geology and Geotechnics, *Pamukkale Üniversitesi Mühendislik Bilimleri Dergisi*.26 (2020) 1373–1378. doi:10.5505/pajes.2020.84584.
- [6] J.D. Hemingway, G.A. Henkes, A disordered kinetic model for clumped isotope bond reordering in carbonates, *Earth and Planetary Science Letters*. 566 (2021) 116962. doi:10.1016/J.EPSL.2021.116962.
- [7] Ç.M. Oral, D. Kapusuz, B. Ercan, Enhanced Vaterite And Aragonite Crystallization At Controlled Ethylene Glycol Concentrations, *Sakarya University Journal of Science*. 23 (1997) 129–138. doi:10.16984/saufenbilder.433985.
- [8] K. Ninagawa, T. Kitahara, S. Toyoda, K. Hayashi, H. Nishido, M. Kinjo, T. Kawana, Thermoluminescence dating of the Ryukyu Limestone, *Quat. Sci. Rev.* 20 (2001) 829–833. doi:10.1016/S0277-3791(00)00058-5.
- [9] J.M. Kalita, M.L. Chithambo, Thermoluminescence and infrared light stimulated luminescence of limestone (CaCO<sub>3</sub>) and its dosimetric features, *Applied Radiation and Isotopes*154(2019).doi:10.1016/J.APRADISO.2019.108888.
- [10] K. Ninagawa, K. Adachi, N. Uchimura, I. Yamamoto, T. Wada, Y. Yamashita, I. Takashima, K. Sekimoto, H. Hasegawa, Thermoluminescence dating of calcite shells in the pectinidae family, *Quaternary Science Reviews*.11 (1992) 121–126. doi:10.1016/0277-3791(92)90052-A.
- [11] J.M. Kalita, G. Wary, X-ray dose response of calcite—A comprehensive analysis for optimal application in TL dosimetry, *Nuclear Instruments and Methods in Physics Research Section B: Beam Interactions with Materials and Atoms*.383(2016)93–102. doi:10.1016/J.NIMB.2016.06.018.
- [12] C. Soliman, S.M. Metwally, Thermoluminescence of the green emission band of calcite, *Radiation Effects and Defects in Solids*. 161(2007)607–613. doi:10.1080/0857647.

- [13] V. Ponnusamy, V. Ramasamy, M. Dheenathayalu, J. Hemalatha, Effect of annealing in thermostimulated luminescence (TSL) on natural blue colour calcite crystals, *Nuclear Instruments and Methods in Physics Research Section B: Beam Interactions with Materials and Atoms*. 217 (2004) 611–620. doi:10.1016/J.NIMB.2003.12.037.
- [14] B. Engin, O. Güven, The effect of heat treatment on the thermoluminescence of naturally-occurring calcites and their use as a gamma-ray dosimeter, *Radiation Measurements*. 32 (2000) 253–272. doi:10.1016/S1350-4487(99)00284-X.
- [15] H.C. del Castillo, J.L.R. Sil, M.A. Álvarez, P. Beneitez, T. Calderón, Relationship between ionoluminescence emission and bond distance (M–O) in carbonates, *Nuclear Instruments and Methods in Physics Research Section B: Beam Interactions with Materials and Atoms*. 249 (2006) 217–220. doi:10.1016/J.NIMB.2006.04.001.
- [16] T. Calderón, P.D. Townsend, P. Beneitez, J. Garcia-Guinea, A. Millán, H.M. Rendell, A. Tookey, M. Urbina, R.A. Wood, Crystal field effects on the thermoluminescence of manganese in carbonate lattices, *Radiation Measurements*. 26 (1996) 719–731. doi:10.1016/S1350-4487(97)82886-7.
- [17] M.R. Khanlary, P.D. Townsend, TL spectra of single crystal and crushed calcite, *Int. J. Radiat. Appl. Instrumentation. Part D. Nucl. Tracks Radiat. Meas.* 18 (1991) 29–35. doi:10.1016/1359-0189(91)90088-Y.
- [18] M.A. Diaz, B.J. Luff, P.D. Townsend, K.R. Wirth, Temperature dependence of luminescence from zircon, calcite, Iceland spar and apatite, *International Journal of Radiation Applications and Instrumentation. Part D. Nuclear Tracks and Radiation Measurements*. 18 (1991) 45–51. doi:10.1016/1359-0189(91)90091-U.
- [19] İ.Ç. Keskin, M.İ. Kati, M. Türemiş, S. Gültekin, S. Üstün, A. Çetin, R. Kibar, X-ray irradiated thermo- and radioluminescence, structural and thermal characterization of septarian (powder&bulk) from Madagascar, *Optical Materials*. (Amst) 83 (2018) 176–181. doi:10.1016/J.OPTMAT.2018.06.005.
- [20] Y. Tuncer Arslanlar, Ç. Keskin, M.İ. Kati, M. Türemiş, A. Çetin, R. Kibar, Investigation on Cathodoluminescence Properties of Copper Implanted ZnO Samples, *Celal Bayar University Journal of Science*. 15 (2019) 145–149. doi:10.18466/cbayarfbe.475150.
- [21] M. Singh, S. Vinodh Kumar, S.A. Waghmare, P.D. Sabale, Aragonite-vaterite-calcite: Polymorphs of CaCO<sub>3</sub> in 7th century CE lime plasters of Alampur group of temples, India, *Construction and Building Materials*. 112 (2016) 386–397. doi:10.1016/J.CONBUILDMAT.2016.02.191.
- [22] M.A. Popescu, R. Isopescu, C. Matei, G. Fagarasan, V. Plesu, Thermal decomposition of calcium carbonate polymorphs precipitated in the presence of ammonia and alkylamines, *Advanced Powder Technology*. 25 (2014) 500–507. doi:10.1016/J.APT.2013.08.003.
- [23] İ.Ç. Keskin, M. Türemiş, M.İ. Kati, R. Kibar, A. Çetin, Effects of CdS quantum dot in polymer nanocomposites: In terms of luminescence, optic, and thermal results, *Radiation Physics and Chemistry*. 156 (2019) 137-143. doi:10.1016/j.radphyschem.2018.11.006.
- [24] A. Çetin, İ. Çetin Keskin, M. Türemiş, M.İ. Kati, B. Taştekin, M.A. Çipiloğlu, R. Kibar, The Investigation of Kinetic Characterization of Sea Salt via Thermoluminescence Method, *Celal Bayar University Journal of Science*. 13 (2017) 845–849. doi:10.18466/cbayarfbe.370366.
- [25] M.İ. Kati, G. Sam, İ.Ç. Keskin, M. Türemiş, A. Çetin, R. Kibar, Pembe Spodümenin Termoluminesans Özelliklerinin İncelenmesi ve Kinetik Parametrelerinin Hesaplanması, *El-Cezeri Journal of Science and Engineering*. 3 (2016) 258-271. doi:10.31202/ecjse.264189.
- [26] M.İ. Kati, K. Kadiroğulları, M. Türemiş, İ.Ç. Keskin, A. Çetin, R. Kibar, The Investigation of Thermoluminescence Properties of Tooth Enamel, *El-Cezeri Journal of Science and Engineering*. 3 (2016) 297–303. doi:10.31202/ecjse.264193.
- [27] S. Gültekin, S. Yıldırım, O. Yılmaz, İ.Ç. Keskin, M.İ. Kati, E. Çelik, Structural and optical properties of SrAl<sub>2</sub>O<sub>4</sub>: Eu<sup>2+</sup>/Dy<sup>3+</sup> phosphors synthesized by flame spray pyrolysis technique, *Journal of Luminescence*. 206 (2019) 59–69. doi:10.1016/J.JLUMIN.2018.10.011.
- [28] M.İ. Kati, İ.Ç. Keskin, M. Türemiş, A. Çetin, R. Kibar, The Role of Eu<sup>3+</sup> Ion on Luminescence, TL Kinetic Parameter and Electrochemical Behaviors of Sr<sub>0.5</sub>Ca<sub>0.5</sub>WO<sub>4</sub> Phosphor Synthesized via Sol-Gel Technique, *El-Cezeri Journal of Science and Engineering*. 8 (2021) 254-267. doi:10.31202/ecjse.833068.
- [29] İ.Ç. Keskin, M.İ. Kati, M. Türemiş, A. Çetin, Y. Tuncer Arslanlar, R. Kibar, Determination of Thermoluminescence Kinetic Parameters of White and Blue Chalcedony Exposed to X-ray Irradiation, *Radiation Physics and Chemistry*. (2018). doi:10.1016/j.radphyschem.2018.05.031.